Supporting information

In-situ TEM observation of phase transition of nanoscopic patterns on baroplastic block copolymer film during nanoindentation

*Ara Jo[†], Gil Ho Gu[‡], Hong Chul Moon[†], Sung Hyun Han[†], Sang Ho Oh[‡], Chan Gyung Park[‡], and Jin Kon Kim[†]**

†National Creative Research Center for Block Copolymer Self-Assembly, Department of Chemical Engineering, Pohang University of Science and Technology (POSTECH), San 31 Hyoja-dong, Pohang 790-784, Republic of Korea ; E-mail: jkkim@postech.ac.kr
‡ Department of Materials Science and Engineering, Pohang University of Science and Technology (POSTECH), San 31 Hyoja-dong, Pohang 790-784, Republic of Korea

S1. Experimental details

Preparation of a PS-b-PnPMA film : A symmetric PS-*b*-PnPMA, having a styrene volume fraction of 0.5 and a number-average molecular weight (Mn) of 54,000, was prepared by anion polymerization. The lamellar spacing (L_o) of PS-*b*-PnPMA was 22 nm measured by synchrotron small angle X-ray scattering. The 6 wt% of PS-*b*-PnPMA solution in toluene was spin-coated onto Pt-coated Si substrate at 4000 rpm for 60 s, and thermally annealed at 120 ^oC for two days which induced the film to have the lamellar microdomains oriented parallel to the substrate. Typical thickness of the film was ~225 nm.

Preparation of a PS-b-PI film : A symmetric PS-*b*-PI having a styrene volume fraction of 0.5 and a number-average molecular weight (Mn) of 24,700 was prepared by anion polymerization. The 6 wt% of PS-*b*-PI solution in toluene was spin-coated onto Si substrate at 4000 rpm for 60 s, and thermally annealed at 120 ^oC for two days which induced the film to have the lamellar microdomains oriented parallel to the substrate. Typical thickness of the film was ~223 nm.

Staining and deposition of protective layer: To obtain clear TEM images, the PS-*b*-PnPMA film was stained with ruthenium tetroxide (RuO_4) for 45 min; thus the dark region appearing in TEM images represents the PS microdomains. The PS-b-PI film was stained with osmium tetroxide (OsO_4) for 90 min; thus the dark region appearing in TEM images represents the PI microdomains. To avoid damage of the top surface of the films during gallium (Ga) ion milling, an Au protective layer with 25 nm thickness was deposited at a rate of 2~2.5Å/s under high vacuum ($3x10^{-6}$ Torr) by thermal evaporator.

FIB processing : To prepare the TEM specimen, a focused ion beam (FIB: SM1 3050, Seiko) instrument was used. Protective layer of carbon was deposited on the polymer film to prevent beam-induced damage during the milling process. Then, the selected area was milled by Ga ions and extracted by an omniprobe mounted inside the FIB chamber. After transfer on a TEM lift-out grid, the mounted polymer sample was finally thinned to have ~150 nm thickness to allow electron transparency. After the FIB-prepared TEM sample was connected to tungsten wire, it was put into a nanoindenter holder.

In-situ TEM Experiment : In-situ TEM Experiment was performed with TEM (JEOL JEM 2100F) working at 200 keV with a nanoindentation holder (Nanofactory^{TM}) having a diamond tip and operating in displacement-controlled mode with a nominal displacement rate of~0.5 nm/s. Videos of indentation process were recorded with a charge-coupled device (CCD) camera (Gatan Orius SC200D; Gatan, Pleasanton) at 40 frames per second.

S2. Removal of the passivation layer

Before the indentation on the polymer film, the passivation layer consisting of carbon and Au was carefully removed by an indenter tip, as schematically shown in Fig S1a. First, a tip is indented onto the polymer surface as shown in Fig S1b. Then, the passivation layer is peeled from the polymer surface by a careful control of the force of the indenter tip as shown in Fig S1c-e. Unless the passivation layer is removed, we could not observe the TEM images clearly during the indentation.

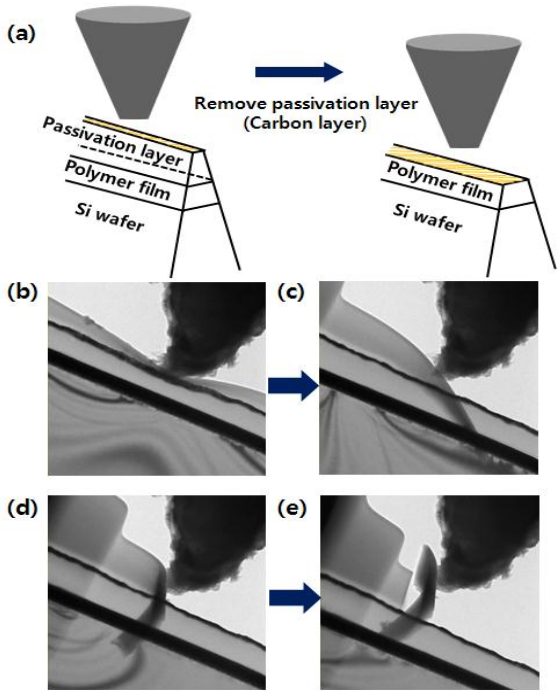

Fig S1. Removal of the passivation layer. (a) Schematic drawing and (b)-(e) Sequential TEM movie frames during the removal of the passivation layer

S3. *Enlarged snap shots from the in-situ TEM movies for PS-b-PnPMA and PS-b-PI before and after indentation.*

To clear demonstrate whether the phase transition occurs or not during nanoindenation, we presented enlarged in-situ TEM movie images before and after indentation for PS-*b*-PnPMA (Fig S2) and PS-*b*-PI (Fig S3). For PS-*b*-PnPMA film, the lamellar microdomains parallel to the substrate were clearly observed before indentation, but these disappeared near indented parts (between red and yellow dotted line in the Figure S2b). On the other hand, well-developed lamellar microdomains in PS-*b*-PI maintained regardless of indentation.

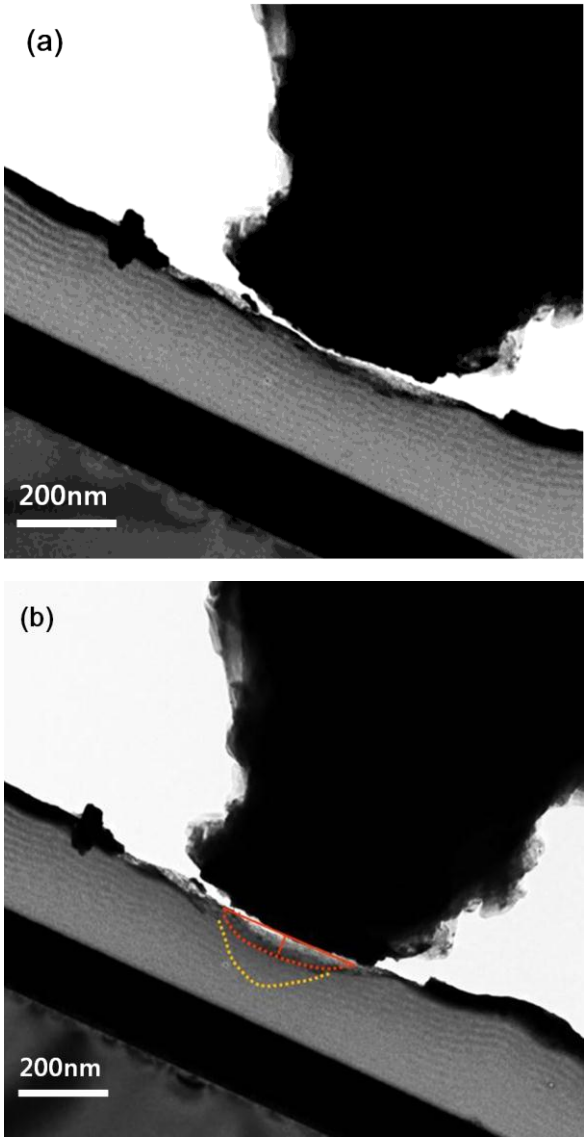

Fig S2. Enlarged *in-situ* TEM movie images for PS-*b*-PnPMA thin film (a) before and (b) after indentation.

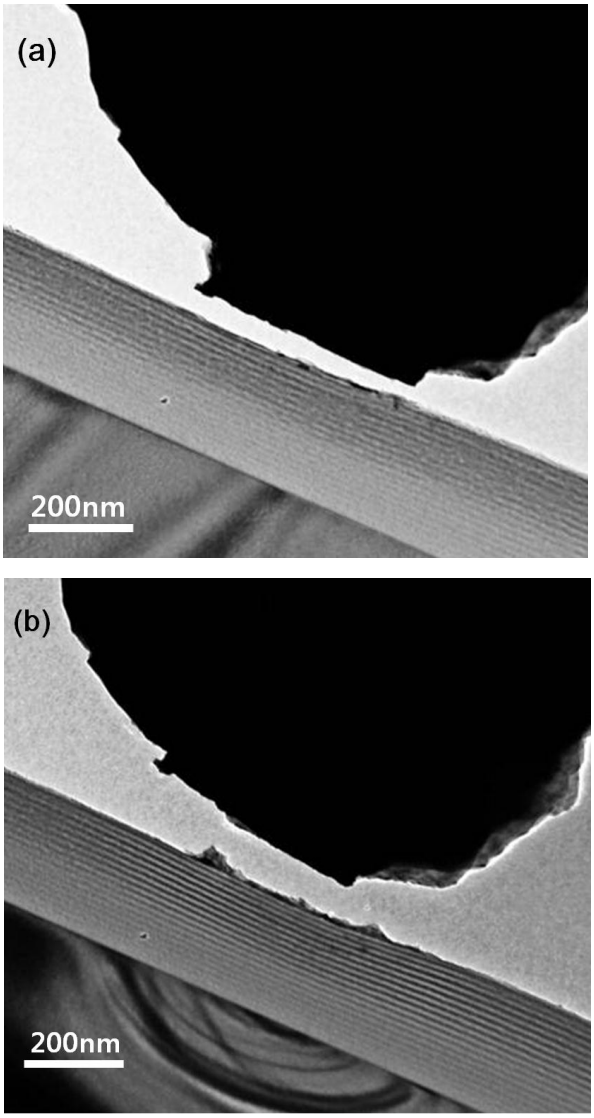

Fig S3. Enlarged *in-situ* TEM movie images for PS-*b*-PI thin film (a) before and (b) after indentation.

S4. *In-situ* nanoindentation experiments for block copolymer thin films without removal of passivation layer

In-situ nanoindentation experiments for block copolymer thin films without removal of the passivation layer are also performed to observe the morphological change by indentation with a larger force. For PS-*b*-PnPMA film, the ordered lamellar microdomains are changed to the disordered state (Fig S4a), and the disordered regions are much wider than those of PS-*b*-PnPMA film without the passivation layer, as shown in Fig S4b-d. Fig S4b-d are TEM images corresponding to the left, the center, the right of the indentation regions. The disordered state is clearly observed at the regions indented by the diamond indenter tip, marked by the dotted line. Fig S4e is the final morphology after the indentation, and Fig. S4f is schematic of the morphology during the indentation.

On the other hand, for PS-*b*-PI film, the disordered region is not observed even at the areas just below the indenter where the pressure (of indentation force) is the largest. That is, the lamellar microdomains under the indenter remained at the maximum force, as shown Fig. S5b. Fig S5d is a schematic of the morphology during indentation.

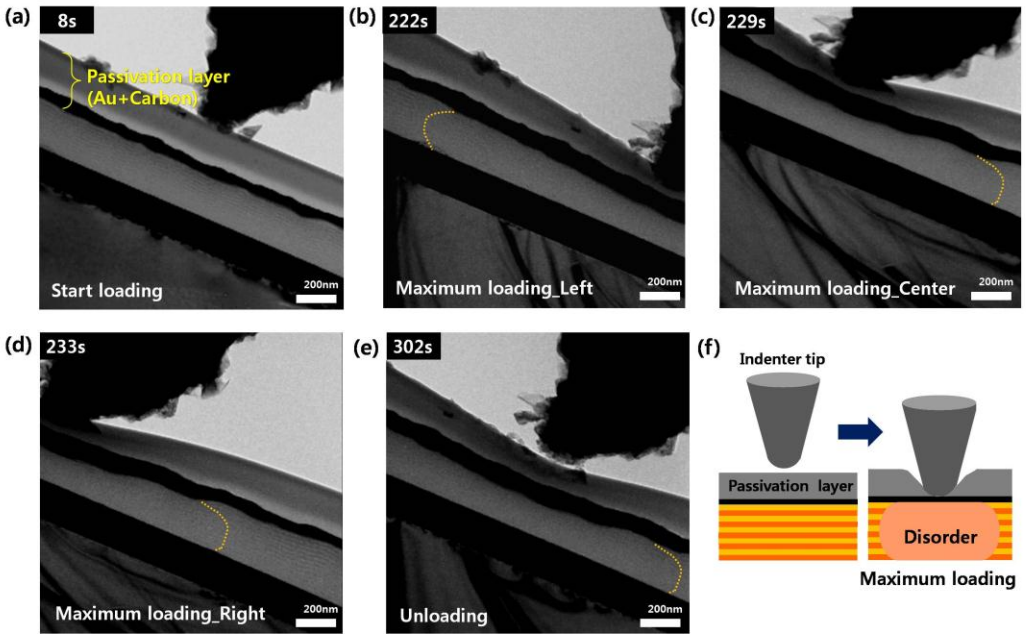

Fig S4. In-situ TEM images during the indentation on PS-*b*-PnPMA film without removal of the passivation layer. (a) t = 8 s (start point of loading), (b) t = 222 s and the left *region of the indented part* at the maximum depth, (c) t = 229 s and the center region of the indented part at the maximum depth, (d) t =233 s and the right region of the indented part at the maximum depth, (e) t = 302s (after complete unloading). (f) schematic of morphological change during the indentation.

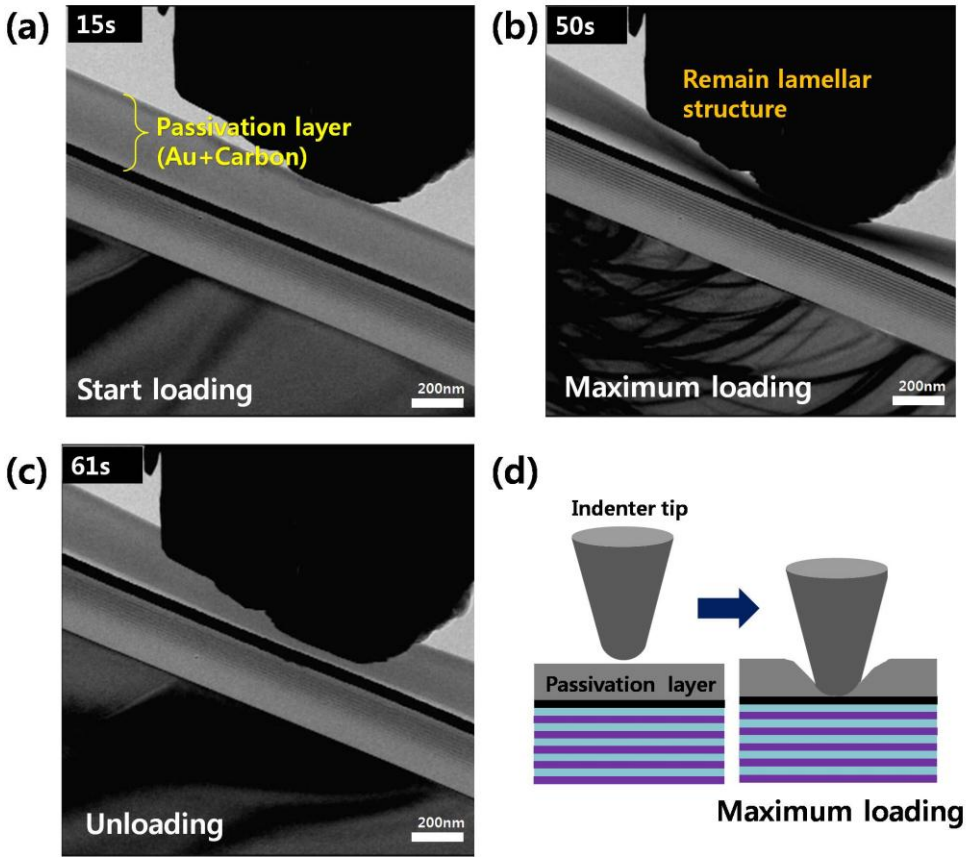

Fig S5. In-situ TEM images during the indentation on the PS-*b*-PI film without removal of the passivation layer. (a) t = 15 s (start point of loading), (b) t = 50 s (the maximum depth), (c) t = 61s (after complete unloading). (d) schematic of morphological change during the indentation.

S5. *Ex-situ TEM images after indentation for PS-b-PnPMA and PS-b-PI thin films.*

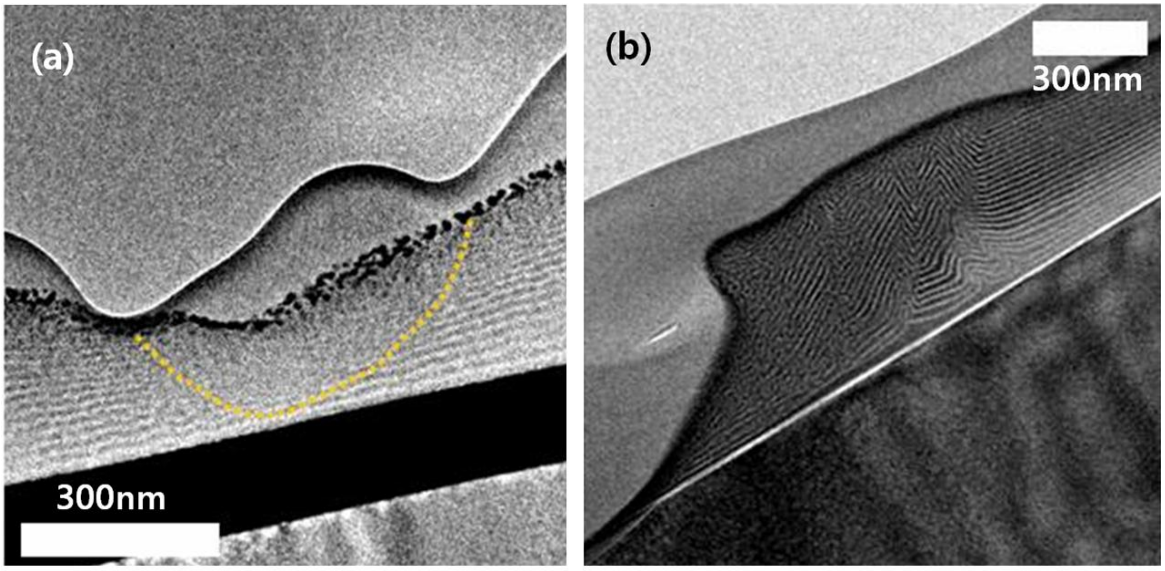

Fig S6. *Ex-situ* TEM images taken from our previous paper[R1] for (a) PS-*b*-PnPMA and (b) PS-*b*-PI thin film after indentation.

When we took *ex-situ* TEM images for both PS-*b*-PnPMA (Fig S6a) and PS-*b*-PI (Fig S6b) after indentation, the phase transition from the lamellar microdomains to disordered state was clearly observed for PS-*b*-PnPMA thin film. However, non-baroplastic PS-*b*-PI film maintained lamellar microdomains in both indented and pile-up regions.

S6. *Effect of staining and Pt coating on the nanostructure and phase transition of PS-b-PnPMA thin films.*

Although selective PS staining by RuO_4 for enhancing TEM image contrast causes chemical bondings, the phase transition for RuO_4-stained PS-*b*-PnPMA thin film was also clearly observed. One possible difference between bare and RuO_4-stained films would be the difference in the loading force to make the nanoindented patterns. As shown in Figure S7, the maximum load for RuO_4-stained film is ~ twice that of bare film. But, when Pt was coated on RuO_4-stained film, the maximum load is almost the same. Furthermore, when we observed the phase transition of RuO4-stained PS-*b*-PnPMA thin film followed by Pt coating and FIB sectioning, the indented area became disordered state, while the non-indented region maintained the lamellar microdomains, as shown in Figure S8. Therefore, we consider that the selective staining or FIB-sectioning did not affect the baroplasticity (or nanostructures) of PS-*b*-PnPMA thin film.

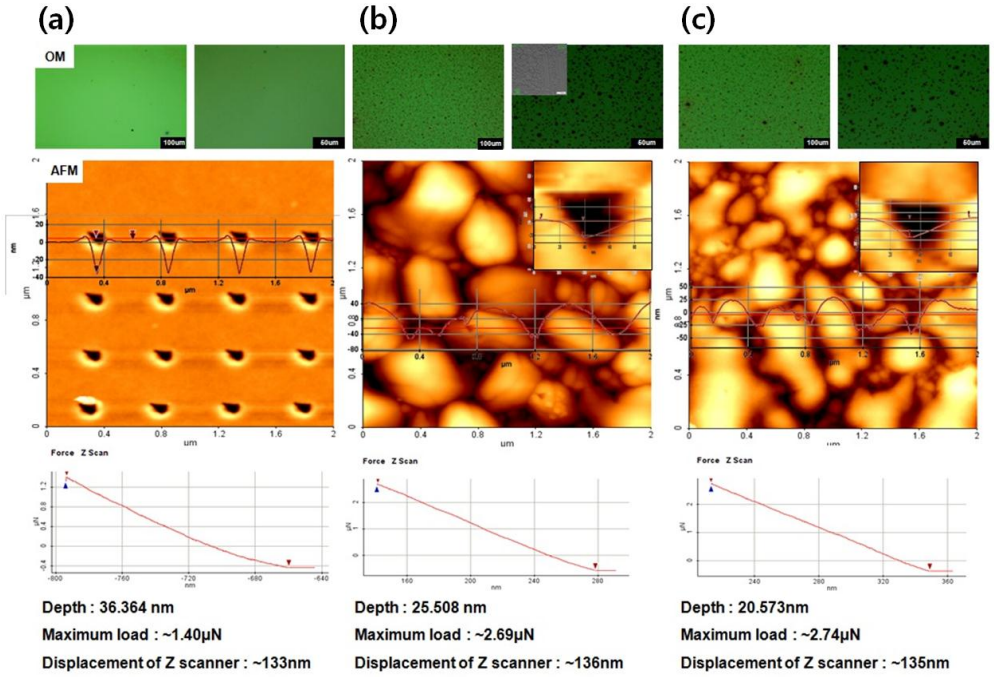

Fig S7. OM (top panel), AFM images (middle panel) and force z-scan (bottom panel) for (a) bare PS-*b*-PnPMA thin film, (b) RuO_4-stained PS-*b*-PnPMA thin film, and (c) RuO_4-stained followed by Pt coating on PS-*b*-PnPMA thin films during indentation.

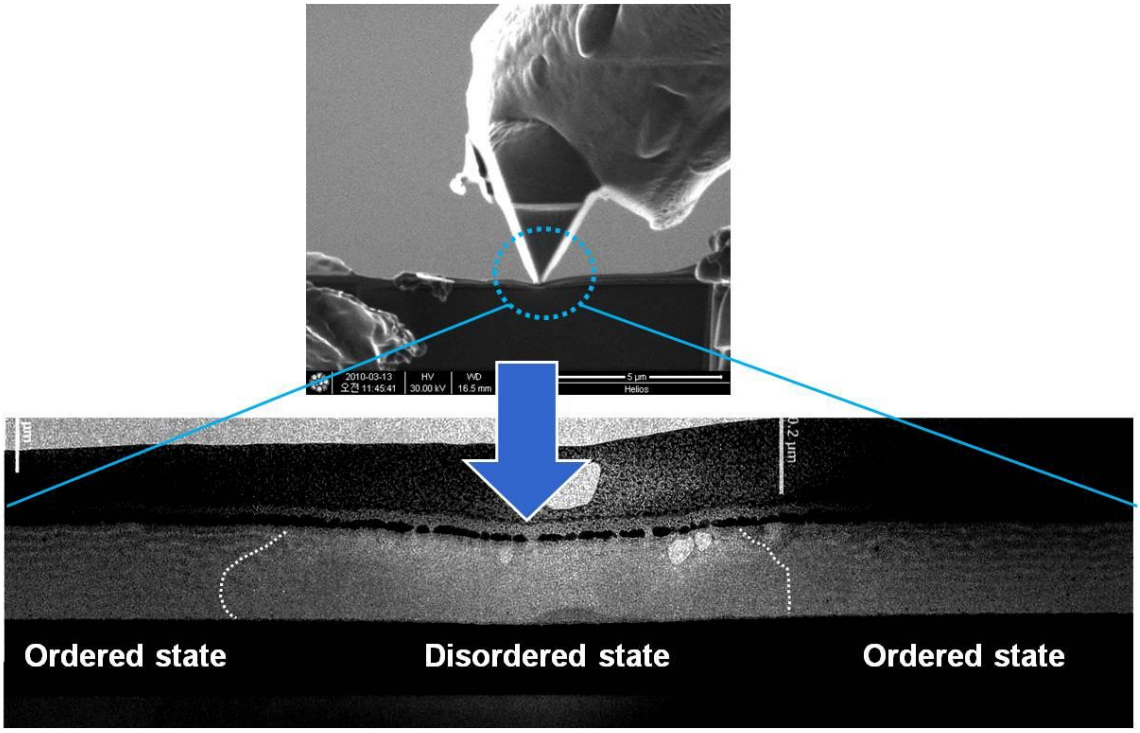

Fig S8. TEM image after indentation for FIB sectioned PS-*b*-PnPMA thin film after RuO_4-staining and Pt coating.

Reference

(R1) A. Jo, W. Joo, W. H. Jin, H. Nam, J. K. Kim, *Nat. Nanotechnol*. 2009, **4**, 727.